Murine model indicates 22q11.2 signaling adaptor *CRKL* is a dosage-sensitive regulator of genitourinary development

Meade Haller[a,b,1], Qianxing Mo[c], Akira Imamoto[d], and Dolores J. Lamb[a,b,1]

[a]Department of Molecular & Cellular Biology, Baylor College of Medicine, Houston, TX 77030; [b]Department of Urology, Baylor College of Medicine, Houston, TX 77030; [c]Department of Medicine, Dan L. Duncan Cancer Center, Baylor College of Medicine, Houston, TX 77030; and [d]The Ben May Department for Cancer Research, University of Chicago, Chicago, IL 60637

Edited by Mary-Claire King, University of Washington, Seattle, WA, and approved April 5, 2017 (received for review December 3, 2016)

The spectrum of congenital anomalies affecting either the upper tract (kidneys and ureters) or lower tract (reproductive organs) of the genitourinary (GU) system are fundamentally linked by the developmental origin of multiple GU tissues, including the kidneys, gonads, and reproductive ductal systems: the intermediate mesoderm. Although ∼31% of DiGeorge/del22q11.2 syndrome patients exhibit GU defects, little focus has been placed on the molecular etiology of GU defects in this syndrome. Among del22q11.2 patients exhibiting GU anomalies, we have mapped the smallest relevant region to only five genes, including *CRKL*. *CRKL* encodes a src-homology adaptor protein implicated in mediating tyrosine kinase signaling, and is expressed in the developing GU-tract in mice and humans. Here we show that *Crkl* mutant embryos exhibit gene dosage-dependent growth restriction, and homozygous mutants exhibit upper GU defects at a microdissection-detectable rate of 23%. RNA-sequencing revealed that 52 genes are differentially regulated in response to uncoupling *Crkl* from its signaling pathways in the developing kidney, including a fivefold up-regulation of *Foxd1*, a known regulator of nephron progenitor differentiation. Additionally, *Crkl* heterozygous adult males exhibit cryptorchidism, lower testis weight, lower sperm count, and subfertility. Together, these data indicate that *CRKL* is intimately involved in normal development of both the upper and lower GU tracts, and disruption of *CRKL* contributes to the high incidence of GU defects associated with deletion at 22q11.2.

del22q11.2 | haploinsufficient | genitourinary | urogenital | congenital defects

Commonly referred to as DiGeorge syndrome, 22q11.2 deletion syndrome affects ∼1 in 4,000 births and is associated with a wide range of developmental abnormalities, including craniofacial, heart, and thymus defects, as well as cognitive deficits and developmental delay (1). Among the less penetrant yet equally detrimental congenital anomalies associated with 22q11.2 deletion are defects of the genitourinary (GU) system affecting ∼31% of patients (2). The clear association of 22q11.2 dosage variation with GU anomalies indicates that one or more genes within the commonly deleted region are involved in the normal development of the GU system. Identifying and characterizing these genes provides valuable information not just for diagnosing and treating patients with clinical DiGeorge syndrome, but potentially a wider spectrum of GU patients harboring mutations within a common signaling network.

Both syndromic and isolated congenital anomalies of the GU tract are common. Lower-tract defects occur at frequencies of ∼5.9% of male births for cryptorchidism (3), 1:240 for hypospadias (4) (USA cohort), and a conservative estimate of 1:4,500 for the less-common defect of ambiguous genitalia (5). Upper-tract defects, commonly referred to as congenital anomalies of the kidney and urinary tract (CAKUT), are also common, affecting 0.3–0.6% of births (6). CAKUT refers to a spectrum of renal defects, including agenesis, hypoplasia, and anomalies of the ureter accounting for 20–30% of all structural birth defects (6). Despite congenital GU anomalies of the upper and lower systems being common, requiring extensive surgical interventions and exhibiting high morbidity and mortality rates, the conditions are often socially stigmatized and the molecular basis of many of these conditions remains largely unknown.

CRKL encodes an adaptor protein with SH2 and SH3 homology domains (7) and has been previously linked to a plethora of signaling pathways in a wide variety of normal and diseased tissues, including PI3K signaling (8, 9), BCR/ABL signaling (10), and FGF signaling (11, 12). *CRKL* lies within the standard deleted region of 22q11.2 patients and was previously linked via murine models to a variety of the congenital malformations associated with the disease, including thymic aplasia, heart defects, and neurocristopathies (13). In 2010, a large-scale array comparative genomic hybridization (aCGH) screen of both syndromic and nonsyndromic patients with GU anomalies further indicated that 22q11.2 copy number variations (CNVs) are associated with GU defects of both the upper and lower tracts (14).

A recent study of 135 murine mutant lines harboring congenital heart disease (CHD) indicated that 29% of CHD mutant lines also harbor CAKUT, indicating mechanistic links between cardiovascular and renal malformations (15). Although not part of the CHD study, *Crkl*-null mice exhibit cardiac outflow anomalies (16) and are therefore more likely to harbor a cooccurrence of GU defects. Indeed, a podocyte-specific model of *Crkl* deletion indicates that *Crkl* and *Crk* are partially redundant in podocytes

Significance

Common deletions affecting multiple genes that cause multiple birth defects can be studied by investigating each gene's independent role in embryonic development. This study shows that a specific gene, *CRKL*, which lies within the commonly deleted region at chromosome locus 22q11.2, is required for normal overall embryonic growth, and normal development of the kidneys and testes. Deletion of only the *Crkl* gene in mice is sufficient to cause increased incidence of birth defects commonly seen in humans who possess deletion at 22q11.2. This study shows that *CRKL* is one of the key genes whose deletion contributes to the urogenital birth defects associated with multiple-gene deletion at chromosome 22q11.2, indicating a new target for gene therapy in affected patients.

Author contributions: M.H. and D.J.L. designed research; M.H. performed research; A.I. and D.J.L. contributed new reagents/analytic tools; M.H., Q.M., and D.J.L. analyzed data; and M.H., Q.M., A.I., and D.J.L. wrote the paper.

The authors declare no conflict of interest.

This article is a PNAS Direct Submission.

[1]To whom correspondence may be addressed. Email: meade.haller@gmail.com or dlamb@bcm.edu.

This article contains supporting information online at www.pnas.org/lookup/suppl/doi:10.1073/pnas.1619523114/-/DCSupplemental.

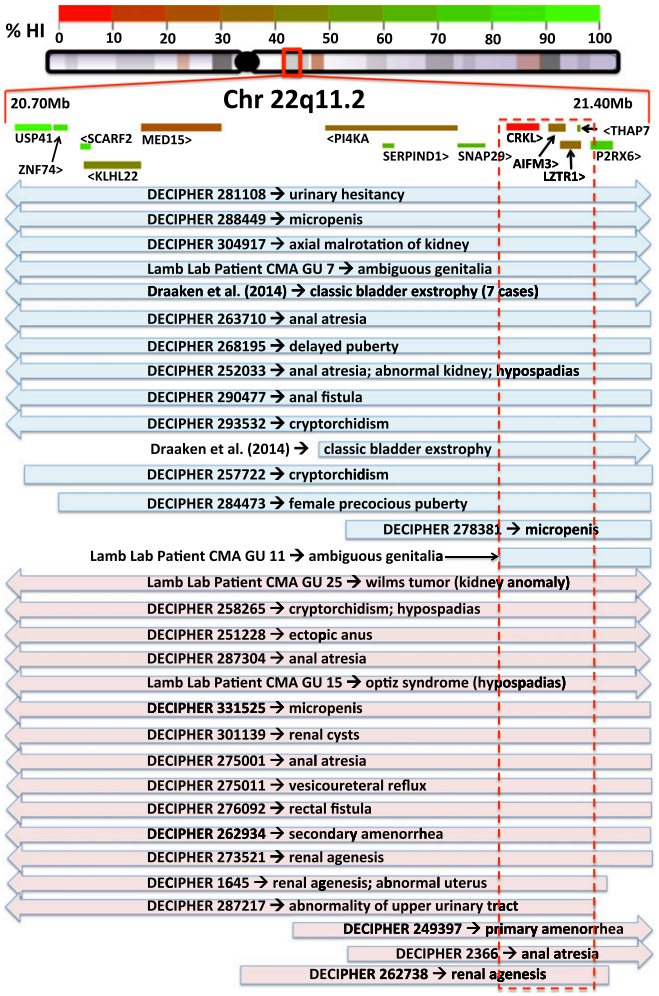

Fig. 1. Map of GU abnormal patients with CNVs covering 22q11.2 indicates *CRKL* as candidate gene. *CRKL* is within the minimal region of overlap and harbors the highest pLI score (pLI = 0.16). Data are gleaned from DECIPHER database, literature (18), as well as original data from D.J.L.'s laboratory (14). Blue indicates duplication; pink indicates deletion. Arrows indicate CNV expands beyond map. Red dotted box indicates minimal region of maximum CNV overlap.

and codeletion results in albuminuria and altered podocyte process architecture (17). The goal of this study is to further our understanding of normal and abnormal GU development on a molecular and genetic level, and improve the diagnosis and treatment of both syndromic and nonsyndromic 22q11.2 variation patients by examining the role of *CRKL* in GU development.

Results

***CRKL* Lies Within the Minimal Region for 22q11.2 Patients with GU Anomalies and Is Expressed During GU Development.** By retrospectively analyzing 22q11.2 patients from the DECIPHER database, previously published literature (18), and patient data acquired from aCGH previously performed by our laboratory (14), we compiled an overlap map of patients with 22q11.2 dosage variation who also exhibit GU phenotypes (Fig. 1). The smallest region covered by all of the mapped GU 22q11.2 CNVs encompasses five protein-coding genes: *CRKL*, *AIFM3*, *LZTR1*, *THAP7*, and *P2RX6*. We referred to the ExAC database of 60,706 individual genomes (exac.broadinstitute.org) to determine the likelihood of haploinsufficiency for each gene (probability of loss-of-function intolerance; pLI score). Of the five genes within the minimal region, *CRKL* harbors the highest pLI score at 0.16. Scores for the other four genes within the minimal region were *AIFM3* pLI = 0, *LZTR1* pLI = 0, *THAP7* pLI = 0.03, and *P2RX6* pLI = 0. Additionally, only two truncating mutations of *CRKL* are reported in the ExAC database, both of which are located at the end of the 303-aa protein sequence: p.Gln297Ter and p.Glu301Ter. The absence of any early truncating mutations in the 60,706 genomes of the ExAC database suggests an unappreciated intolerance to loss-of-function mutations in *CRKL*.

An aCGH and CNV qPCR screen showed duplications ($n = 2$) and deletions ($n = 2$) encompassing *CRKL* (Fig. 1, "Lamb Lab Patients") were enriched in a population of GU-abnormal patients and present at 1.4% ($n = 277$; $P = 0.0004$) compared with the unselected general population where *CRKL*-encompassing CNVs are present at 0.088% (6 of 6,813; only duplications found) (19). CNVs in *CRKL* are also enriched in our cohort of GU-abnormal patients compared with rates in the generally disease-enriched cohort of the ExAC database (19 deletions; 47 duplications; 66 of 60,706; 0.1%; all analyzed ethnic subgroups represented; $P = 0.03$). Our laboratory's cohort of GU-abnormal patients is heavily biased toward lower-tract defects, and our findings may underestimate the frequency of *CRKL* encompassing CNVs in GU-abnormal patients because of underrepresentation of patients with upper-tract phenotypes.

To define *Crkl* expression in the developing GU system to ask whether these observed CNVs might contribute to GU defects associated with 22q11.2 dosage variation, in situ hybridization was performed on murine tissues (Fig. 2 *A*–*F*), as well as a qPCR screen of human fetal cDNAs from various tissues (Fig. 2*G*). *Crkl* is expressed throughout the developing mouse at modest levels (Fig. 2*A*), and at moderate levels in the developing GU tract with emphasis on the E12.5 genital tubercle (Fig. 2*B*, red dotted outline) and the E16.5 kidneys, bladder, and testis (Fig. 2*C*). E16.5 *Crkl* expression patterns are largely corroborated by E15.5 data from the GUDMAP database (www.gudmap.org; entry #10685). Human *CRKL* is expressed throughout a variety of fetal tissues, including liver, lung, and skeletal muscle, and, importantly for DiGeorge syndrome phenotypes, heart, spleen, thymus, brain, and kidney (Fig. 2*G*). *CRKL* is expressed in the human fetal kidney at levels comparable to or higher than human fetal organs affected in *Crkl* murine deletion models (thymus and heart, respectively).

Loss of *Crkl* Adapter Functions Mimics Null-Deletion Models and Indicates Haploinsufficiency via Dose-Dependent Intrauterine Growth Restriction in Mice. To determine a role that *Crkl* may play in GU development as implicated above, we used a cre-dependent

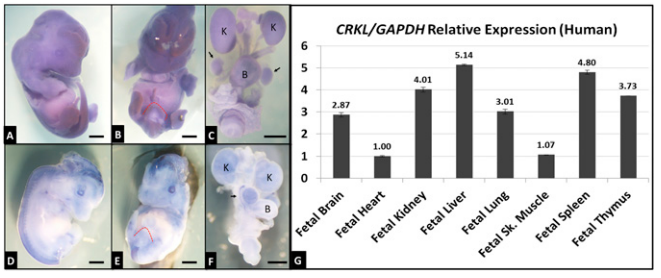

Fig. 2. Murine *Crkl* and human *CRKL* expression patterns. *Crkl* antisense (*A*–*C*) and sense control (*D*–*F*) probes were used to stain E12.5 (*A*, *B*, *D*, and *E*) whole embryos and E16.5 isolated GU tracts (*C* and *F*). Blue areas indicate probe hybridization. *Crkl* is expressed at moderate levels (higher than sense probe background) throughout the developing embryo, including genital tubercle (red dotted outline), kidneys (K), bladder (B), and testes (black arrows). (Scale bars, 2 mm.) *CRKL* qPCR was performed on cDNAs (*G*) from spontaneously aborted human fetuses. Expression levels of tissues shown relative to heart expression. Error bars represent SEM.

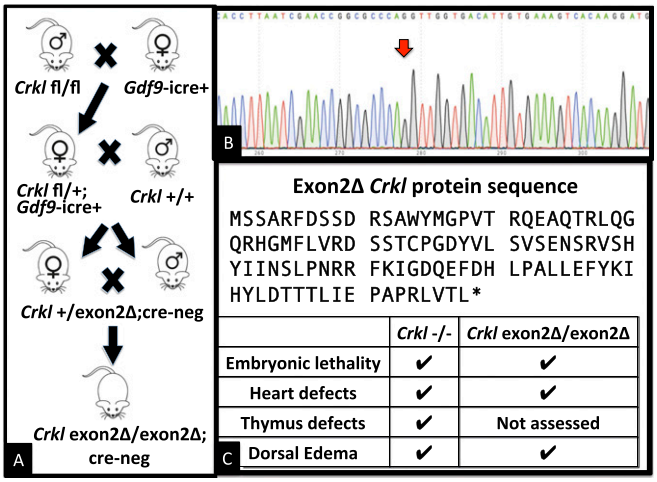

Fig. 3. Generation of *Crkl* exon2Δ/exon2Δ embryos. (*A*) A multigenerational cross was used to generate *Crkl* exon2Δ/exon2Δ embryos. (*B*) Deletion was validated by Sanger sequencing of cDNA indicating splicing of exon 1 to exon 3 (red arrow). (*C*) Exon 2-deleted protein sequence showing premature stop, and *Inset* chart comparing predominant phenotypes of $Crkl^{-/-}$ to *Crkl* exon2Δ/exon2Δ.

conditional allele in which exon 2 of murine *Crkl* is flanked by two loxP sites. The second exon of *Crkl* encodes the SH3n domain and a short portion of the SH3c domain. The remainder of the SH3c domain is encoded in the third exon, which is transcribed but not translated in cre-recombined tissues because of the introduction of a premature stop codon. *Crkl* exon2Δ/exon2Δ embryos were produced using a three-generation cross between *Crkl* exon2 fl/fl and GDF9-icre oocyte-specific cre-recombinase mice (Fig. 3*A*). Upon generation of full-bodied *Crkl* exon2Δ/exon2Δ embryos, RNA was isolated from E16.5 kidneys and cDNA was sequenced with Sanger sequencing to validate splicing of *Crkl* exon 1 to exon 3 (Fig. 3*B*). *Crkl* exon2Δ/exon2Δ animals are embryonic-lethal at E18.5 with no recovery of live null animals perinatally suggesting a tight phenocopy of the $Crkl^{-/-}$ embryos developed and assessed previously (Fig. 3*C*) (11, 13). Upon analysis of mutant embryos it was immediately apparent that both *Crkl* exon2Δ/exon2Δ as well as *Crkl*+/exon2Δ embryos exhibit intrauterine growth restriction (Fig. 4 *A* and *B*). Because loss of a single copy of wild-type *Crkl* is sufficient to cause restricted intrauterine growth, *Crkl* is haploinsufficient for normal embryonic development and is likely to contribute to growth restriction associated with 22q11.2 deletion in humans (20).

Murine Loss of *Crkl* Exon 2 Results in 23% Incidence of Upper GU-Tract Embryonic Phenotypes. *Crkl* exon2Δ/exon2Δ embryos and their control littermates were analyzed by microdissection for overt GU structural anomalies. A total of 242 embryos were analyzed and upper tract GU phenotypes including hydronephrosis (Fig. 4 *C*, *D*, and *F*) and unilateral renal agenesis (Fig. 4*E*) were found in 23% (12 of 52) of *Crkl* exon2Δ/exon2Δ embryos, and not present in 63 $Crkl^{+/+}$ and 127 *Crkl*+/exon2Δ littermates (Fig. 4, *Inset* chart). This incidence is considered statistically significant by Fisher's exact test between *Crkl* exon2Δ/exon2Δ and $Crkl^{+/+}$, with $P = 0.0001$. No overt embryonic phenotypes were present in other microdissected GU tissues, including bladder, gonads, reproductive ducts, and genital tubercle. Because embryos were assessed only for overt structural anomalies, the incidence described here likely underrepresents the true incidence of renal phenotypes in *Crkl*-deficient embryos. Vesicoureteral reflux (VUR) assay on 52 adult male *Crkl*+/exon2Δ and 57 wild-type controls (Fig. S1) revealed a higher-trending but statistically nonsignificant ($P = 0.19$ by Fisher exact test) rate of VUR in 32.7% (17 of 52) of *Crkl*+/exon2Δ males versus 21% (12 of 57) of $Crkl^{+/+}$ controls. Heterozygous mutants exhibited normal bladder capacity normalized to body weight (Fig. S2) and no anomalies of the bladder. Although embryonic and early postnatal VUR studies in other backgrounds indicate wild-type incidences ranging from 0 to 59% (21–23), and embryonic and early postnatal VUR in C57/BL6 occurs at low rates (24, 25), this is the largest study to date showing background incidence of VUR in C57/BL6 adult age-matched males. One of the 52 *Crkl*+/exon2Δ mutants assayed for VUR exhibited unilateral cystic kidney and apparent ureteropelvic junction (UPJ) obstruction as assessed by micro-CT scanning (Fig. S3).

***Crkl* Facilitates Renal Signaling Pathways Affecting a Minimum of 52 Transcripts.** Because *Crkl* facilitates the transduction of a wide variety of signaling pathways in an even wider variety of cell types, it is imperative to our understanding of *Crkl* function specific to renal development to attempt to address which pathways are aberrantly affected when *Crkl* cannot perform its normal adaptor functions within developing kidney tissue. To address this question, mRNA from $n \geq 3$ E16.5 kidney pairs of phenotypically normal *Crkl* exon2Δ/exon2Δ male embryos and $Crkl^{+/+}$ male control embryos was next-generation sequenced at 80 million reads per sample. Phenotypically normal kidneys were used so as to isolate transcript changes primary to *Crkl* dosage variation and exclude transcript differences secondary to organ stress. Fifty-two transcripts are differentially expressed when *Crkl* is uncoupled from its transduction networks in embryonic renal tissue, with a heavy bias toward genes becoming aberrantly up-regulated. This finding suggests that a main function of *Crkl* in the developing kidney is to aid in maintaining suppression of a wide panel of transcripts (Fig. 5). Because of the evidence for *Crkl* haploinsufficiency in intrauterine growth, we also sequenced RNA from *Crkl*+/exon2Δ embryonic kidneys and found that although similar genes are affected in the comparison between *Crkl*+/exon2Δ kidneys and *Crkl* exon2Δ/exon2Δ kidneys (Fig. S4), *Crkl*+/exon2Δ kidney transcripts did not vary from $Crkl^{+/+}$ (Datasets S1–S4). This result correlates with the finding that although *Crkl* is haploinsufficient for intrauterine growth, *Crkl*+/exon2Δ embryos do not exhibit increased incidence of overt upper-tract GU phenotypes. To validate the RNA-seq findings, qPCR was performed on cDNA reverse-transcribed from the RNA samples. Fourteen genes were

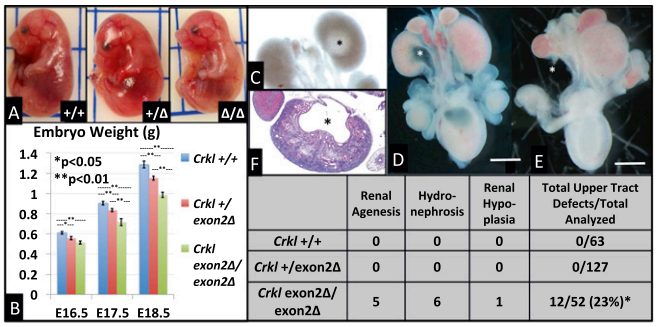

Fig. 4. *Crkl* exon 2 deletion results in dose-dependent intrauterine growth restriction and *Crkl* exon2Δ/exon2Δ embryos exhibit 23% incidence of upper-tract phenotypes. $Crkl^{+/+}$, *Crkl*+/exon2Δ, and *Crkl* exon2Δ/exon2Δ embryos were collected at E16.5 (*A*), E17.5, and E18.5. Loss of one copy of wild-type *Crkl* is sufficient to confer intrauterine growth restriction as early as E16.5 (*B*). *n* for each group ≥ 7. Error bars represent SEM. GU tracts were microdissected from E16–E18. Upper-tract phenotypes were observed and penetrance documented (*Inset* chart). Phenotypes included mild (*C*) to moderate (*D* and *F*) hydronephrosis, unilateral renal agenesis (*E*), and unilateral renal hypoplasia. Asterisks indicate abnormalities. Asterisk in table indicates $P < 0.05$ by Fisher exact test. (Scale bars, 2 mm.)

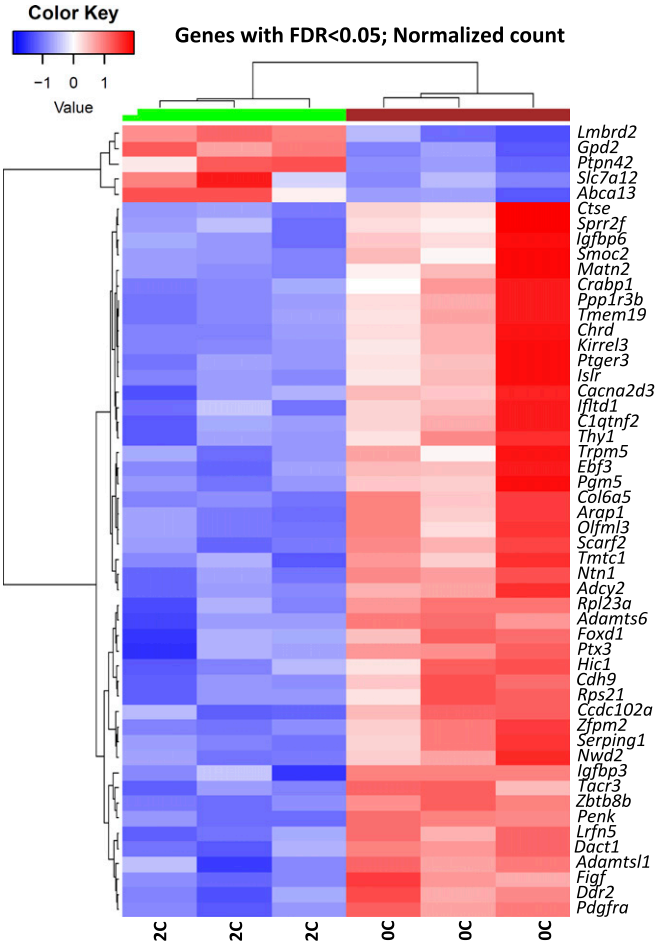

Fig. 5. Fifty-two genes are differentially expressed in *Crkl* exon2Δ/exon2Δ E16.5 kidneys compared with *Crkl*$^{+/+}$ E16.5 kidneys at a normalized false-discovery rate (FDR) < 0.05. Total RNA collected from E16.5 kidneys was extracted and next-generation sequenced. 2C indicates two copies of wild-type *Crkl*; 0C indicates zero copies of wild-type *Crkl*.

selected for validation, several of which are involved in renal development (Fig. 6). Of the validated genes, *Foxd1* is the most significantly affected and exhibits a 5.5-fold induction when *Crkl* is uncoupled from its renal signaling networks. The same cohort of genes was tested for differences between wild-type and heterozygous mutant samples, but no differences were found (Fig. S5).

Adult *Crkl* Exon 2 Deletion Heterozygotes Exhibit Lower-Tract GU Defects and Subfertility. As we were performing our crosses to derive *Crkl* exon2Δ/exon2Δ embryos and maintain the mutant colony, it became apparent that *Crkl*+/exon2Δ males frequently exhibited lower-than-average pups per litter when crossed to wild-type females, and often would become infertile earlier than their male wild-type littermates. To quantify this observation, a two-branched approach to analyze anatomical and physiological lower-tract GU phenotypes was used. To address anatomical defects, testicular parameters of males and controls (n = 11 per group) were defined at the age of observed subfertility onset (~20 wk). To address physiological defects, an age-matched fertility study of n = 11 breeding cages per group across three consecutive litters with breeding starting at 11 wk of age when fertility of mutants was comparable to wild-types was undertaken. *Crkl*+/exon2Δ males exhibit a high penetrance of cryptorchidism (Fig. 7 *A* and *D*), smaller testes and lower testis-to-body-weight ratio (Fig. 7 *B* and *E*), lower sperm concentration (Fig. 7*F*), and abnormal testicular histology (Fig. 7*C*) compared with *Crkl*$^{+/+}$ age-matched controls. Physiologically, *Crkl*+/exon2Δ males sire ~30% fewer pups per litter than *Crkl*$^{+/+}$ controls after their first litter, which is of normal size (Fig. 7*G*). All *Crkl*+/exon2Δ male mice tested produced at least one litter, and two of the experimental breeding cages stopped producing litters at or before their third litter. Approximately even numbers of *Crkl*$^{+/+}$ and *Crkl*+/exon2Δ pups were recovered from experimental cages; this indicates that a potential loss of mutant embryos does not account for the lower pups per litter observed in experimental cages. Additionally, time between litters is unaffected (Fig. S6), indicating that although subfertile by their second litter, *Crkl*+/exon2Δ males are breeding at rates comparable to wild-type controls. Sperm motility was also unaffected (Fig. S7). Based on these findings, *Crkl*+/exon2Δ males exhibit age-related subfertility secondary to testicular atresia. Because the histological findings vary from that typically expected for cryptorchid testicular histology (26,27), the histology observed is likely primary to a role of *Crkl* in adult testicular function rather than secondary to cryptorchidism. These data indicate that *Crkl* is haploinsufficient for murine male fertility, and *CRKL* mutations may play a role in age-related subfertility and infertility in humans. Additionally, subfertility was observed in *Crkl*+/exon2Δ females (Fig. S8). It is important to note that female subfertility is not a result of oocyte malfunction, because females with exon 2 deleted specifically in oocytes (*Crkl* fl/fl;*Gdf9*-icre+) produced viable full-bodied *Crkl*+/exon2Δ offspring when mated to wild-type males.

Discussion

The finding that unrelated, seemingly nonsyndromic patients with congenital GU defects exhibit CNVs clustering at 22q11.2 was, perhaps, not surprising given the fact that 22q11.2 dosage variation is a notoriously complex disease with high phenotypic variability and incomplete penetrance across phenotypes. Genetically complex disorders such as these require simplification to be understood. Deletion and overexpression models of individual genes within large copy-variant genomic loci are indispensable tools to unveiling the effect of each gene's individual impact on a given CNV syndrome. Deletion of murine *Crkl* by our group (exon 2) and others (11, 13, 17) (null and conditional models) revealed that *Crkl* plays a pivotal role in the proper development of a wide variety of tissues whose structures and functions are deleteriously affected in 22q11.2 patients. The mouse model described in this

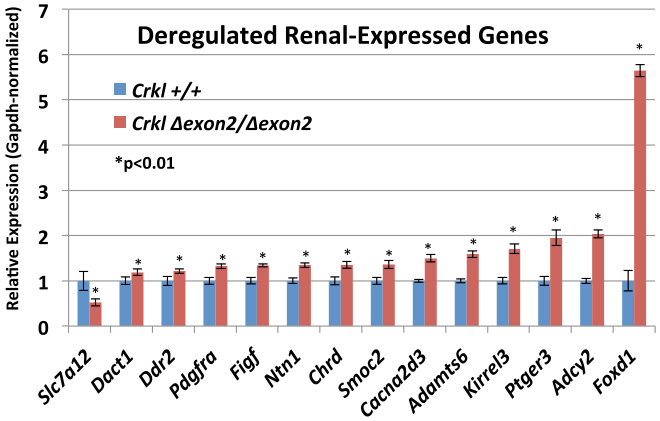

Fig. 6. A subset of genes differentially expressed by RNA-sequencing were chosen to be validated by qPCR. RNAs from the same samples used for sequencing were reverse-transcribed and used to validate differential expression via the higher sensitivity TaqMan qPCR assay. Most of the validated genes showed more robust fold change values by qPCR than indicated by RNA-seq analysis. Error bars represent SEM.

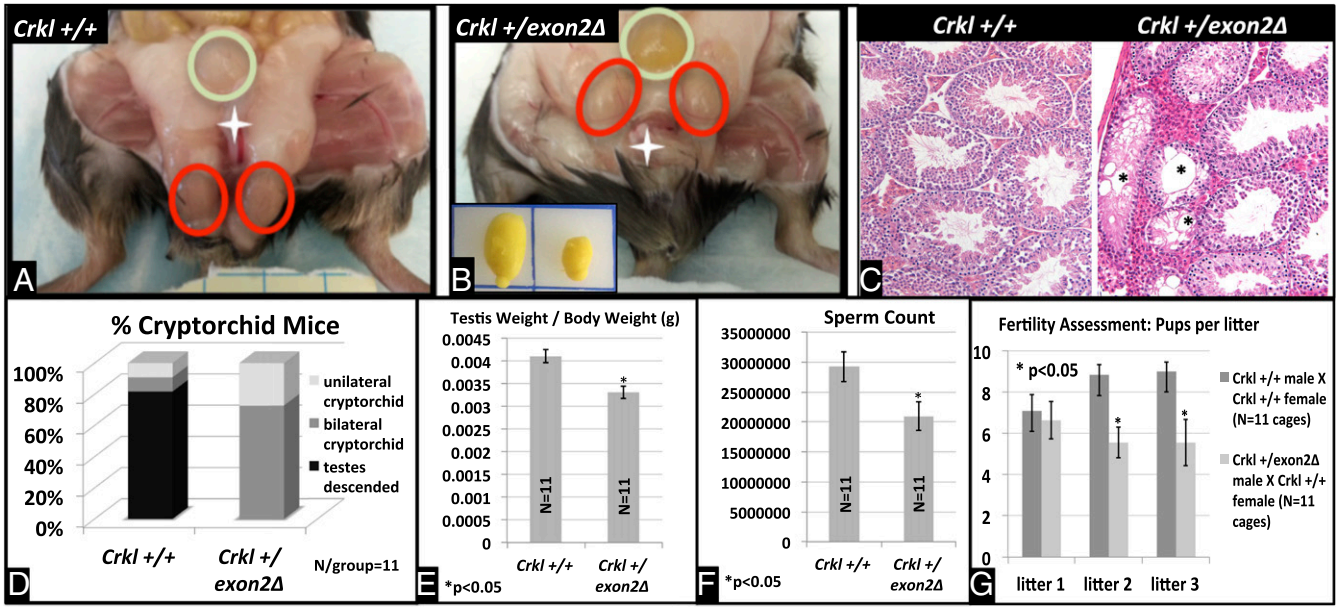

Fig. 7. *Crkl*+/exon2Δ males exhibit cryptorchidism, smaller testes, fewer sperm, and subfertility compared with $Crkl^{+/+}$ controls. Eighteen- to 20-wk-old males ($n = 11$ per group) were analyzed for cryptorchidism (*A*) (testicles circled in red; bladder in green, penis indicated by white star), testicular size (*B*) (*Inset*: *Left* wild-type, *Right Crkl*+/exon2Δ). H&E staining of testes (*C*) confirmed abnormal testicular histology in approximately half of the *Crkl*+/exon2Δ seminiferous tubules with atresia and vacuolization of tubules apparent (*). (Magnification, 10×.) Distribution of cryptorchidism was graphed (*D*). Testicle weight was graphed as a proportion of body weight (*E*). Genotype-blinded sperm count was assessed by hemacytometry (*F*). $n = 11$ cages per group were mated at 11 wk of age and assessed for fertility across three litters (*G*). Error bars represent SEM.

paper shows that in addition to neural, heart, and thymic congenital defects, loss of *Crkl* also contributes to the GU defects characteristic of DiGeorge syndrome, and lends insight to the observation that similar GU anomalies are seen in a subset of nonsyndromic patients with smaller 22q11.2 aberrations.

Although not every phenotypic parameter was compared, the full-body *Crkl* exon 2 deletion model suggests that loss of exon 2 is sufficient to phenocopy a true null allele. This study indicates that loss of one copy of wild-type *Crkl* is sufficient to confer intrauterine growth restriction and adult testicular phenotypes, implicating that *Crkl* is haploinsufficient for a subset of biological structures and functions. This is especially important in the context of 22q11.2 deletions because patients generally still harbor one normal copy of each of the affected genes, rendering them functionally heterozygous. One of the main evolutionary benefits to a biallelic genome is the general unlikelihood that having only one copy of a given gene results in the generation of insufficient amounts of protein to perform that protein's baseline function. In this sense, the second copy of a gene is conventionally thought to represent a backup of all of the data required for that particular genetic program to function. Although haploinsufficient genes are still considered rare, genes are regularly discovered to be dosage-sensitive, and clinically phenotypic syndromes associated with the monoallelic loss of a subset of genes point us in the direction of genes that are haploinsufficient for the development or function of tissues affected in a particular syndrome. In the case of *Crkl*, it appears that one wild-type copy is insufficient to sustain normal embryonic growth as well as normal adult testicular histology and function. Together, these findings suggest that patients with DiGeorge syndrome or smaller aberrations to the *CRKL* gene affecting one or both copies are more likely to exhibit embryonic growth restriction and subfertility in males as adults.

Similar to the high phenotypic variability and incomplete penetrance observed in 22q11.2 deletion patients, our *Crkl* exon 2 deletion mice exhibited partially penetrant congenital renal and ureteral anomalies, ranging from congenital hydronephrosis to unilateral renal hypoplasia and agenesis. The renal agenesis observed uniformly involved apparently normal ureteric growth (Fig. 4*E*), implying that the renal aplasia resultant from *Crkl* exon 2 deletion is secondary to impaired metanephric mesenchyme induction or response rather than aplasia of the ureteric bud. RNA-sequencing of *Crkl* exon 2-deleted embryonic kidneys revealed deregulation of 52 transcripts compared with wild-type controls, with a heavy bias toward transcript induction. This induction bias suggests that in the normal embryonic kidney, *Crkl* facilitates the maintenance of repression signaling across a variety of transcripts. One of the most heavily up-regulated renal genes in response to *Crkl* exon 2 deletion from the panel chosen for validation is *Foxd1*. *Foxd1* is a transcription factor that promotes nephron progenitor differentiation (28). It is unclear whether overexpression of *Foxd1* is detrimental to renal development; however, *Foxd1* duplication is associated with branchial defects (29), which are also common phenotypes observed in 22q11.2 deletion (30). Another gene up-regulated in renal tissue in response to *Crkl* exon2 deletion is *Adcy2*. *Adcy2* encodes adenylyl cyclase 2, an enzyme responsible for catalyzing the production of the signaling molecule cAMP in a wide range of tissues (31). A review of the DECIPHER database shows a correlation between CNVs (both deletions and duplications) covering *ADCY2* and GU phenotypes, including hydronephrosis and ureteral atresia (patient 259229), VUR (patient 262907), and cryptorchidism (patients 279259 and 284051), and previous work has linked *ADCY2* CNVs to abnormalities of the GU tract (14).

From these studies several conclusions can be drawn regarding the role of *Crkl* in GU development, as well as the role of exon 2 in *Crkl* function. Because the *Crkl* exon 2 deletion embryos closely mimic phenotypes observed in *Crkl*-null models, exon 2 deletion, despite producing a truncated protein from translation of exon 1, is most likely a complete loss-of-function mutation. However, it is yet possible that the truncated protein produced by exclusive deletion of *Crkl* exon 2 may retain some function, allowing overt renal phenotypes to persist only in homozygous but not heterozygous murine mutants; this could explain the discrepancy between renal phenotypes being present in

humans heterozygous for 22q11.2 deletion but absent at the microdissection-level in *Crkl*+/exon2Δ mice. Another explanation could be that heterozygous phenotypes are less penetrant, less severe, and therefore not easily detectable by embryonic microdissection. Indeed, a recent study indicates that subtler, histologically detectable phenotypes are penetrant at low levels in *Crkl*+/exon2Δ embryos (32). Because loss of *Crkl* results in dose-dependent intrauterine growth restriction, and because heterozygous animals exhibit high rates of cryptorchidism and subfertility, it can be concluded that *Crkl* is a haploinsufficient gene for a subset of developmental processes. Additionally, it can be concluded that loss of both copies of wild-type *Crkl* confers increased susceptibility to structurally overt upper-tract GU defects. In this same vein, one can hypothesize that loss of a single wild-type copy of *CRKL*, perhaps by itself but especially in combination with modifying genetic aberrations, may be sufficient to induce CAKUT phenotypes of varying severity in patients with 22q11.2 deletion. Additionally, RNA sequencing identified several candidate pathways by which loss of *Crkl* may induce renal phenotypes. These candidate pathways will need to be further studied to narrow down the molecular means by which *Crkl* aberrations affect renal development and function. DiGeorge syndrome is among the many syndromic CNVs that can be screened for embryonically. These technological advances allow researchers to hypothesize that by combining molecular and genetic findings with embryonic screening of at-risk pregnancies, eventually it may be possible to manufacture molecular modifiers to help modulate the effects of syndromic CNVs in utero without undertaking the higher-risk tasks of modifying the embryonic genome or performing infant or in utero surgeries.

Materials and Methods

CNV qPCR of GU-abnormal patients was performed by isolation of genomic DNA from blood followed by CNV qPCR using 20-ng input template in triplicate and TaqMan CNV probe HS02102421, with informed consent from patients and Institutional Review Board approval from the Baylor College of Medicine. C. M. Vezina laboratory protocol (33) was used for in situ hybridization. Takara Clontech Human fetal cDNA panel Cat. 636747 was used with *CRKL* TaqMan probe HS00178304_m1 to determine human expression. *Gdf9*-icre females (34) (Jax stock #011062) were bred to *Crkl* fl/fl to generate *Crkl* exon2Δ mutants. Mutant cDNA was sequenced for validation. Embryonic GU tracts were microdissected for anatomical assessment. RNA from $n \geq 3$ male E16.5 kidneys per genotype was sequenced and reads were mapped, analyzed, and a subset was validated by qPCR. Age-matched males were assessed for testicular parameters and prospective fertility study with endpoint of pups per litter. All mouse work was performed in strict concordance to animal protocols approved by the Institutional Animal Care and Use Committee of the University of Chicago, as well as Baylor College of Medicine. Please refer to *SI Materials and Methods* files for detailed materials and methods and Fig. S9 for RNA-sequencing samples and read quality.

ACKNOWLEDGMENTS. We thank Cenk Cengiz for performing genotype-blinded sperm counts and Marisol O'Neill for performing micro-CT. Portions of this project were made possible by the Baylor College of Medicine Genomic and RNA Profiling (GARP) Core and the UC Transgenics/ES Technology Core. This work was funded by NIH Grants T32DK007763 and R01DK078121.

1. Oskarsdóttir S, Vujic M, Fasth A (2004) Incidence and prevalence of the 22q11 deletion syndrome: A population-based study in western Sweden. *Arch Dis Child* 89:148–151.
2. Wu HY, et al. (2002) Genitourinary malformations in chromosome 22q11.2 deletion. *J Urol* 168:2564–2565.
3. Acerini CL, Miles HL, Dunger DB, Ong KK, Hughes IA (2009) The descriptive epidemiology of congenital and acquired cryptorchidism in a UK infant cohort. *Arch Dis Child* 94:868–872.
4. Springer A, van den Heijkant M, Baumann S (2016) Worldwide prevalence of hypospadias. *J Pediatr Urol* 12:152.e1–152.e7.
5. Hughes IA, Houk C, Ahmed SF, Lee PA; LWPES Consensus Group; ESPE Consensus Group (2006) Consensus statement on management of intersex disorders. *Arch Dis Child* 91:554–563.
6. Nicolaou N, Renkema KY, Bongers EMHF, Giles RH, Knoers NVAM (2015) Genetic, environmental, and epigenetic factors involved in CAKUT. *Nat Rev Nephrol* 11:720–731.
7. ten Hoeve J, et al. (1994) Cellular interactions of CRKL, and SH2-SH3 adaptor protein. *Cancer Res* 54:2563–2567.
8. Segovis CM, et al. (2009) PI3K links NKG2D signaling to a CrkL pathway involved in natural killer cell adhesion, polarity, and granule secretion. *J Immunol* 182:6933–6942.
9. Lian X, et al. (2015) CrkL regulates SDF-1-induced breast cancer biology through balancing Erk1/2 and PI3K/Akt pathways. *Med Oncol* 32:411.
10. Senechal K, Halpern J, Sawyers CL (1996) The CRKL adaptor protein transforms fibroblasts and functions in transformation by the BCR-ABL oncogene. *J Biol Chem* 271: 23255–23261.
11. Moon AM, et al. (2006) Crkl deficiency disrupts Fgf8 signaling in a mouse model of 22q11 deletion syndromes. *Dev Cell* 10:71–80.
12. Seo J-H, Suenaga A, Hatakeyama M, Taiji M, Imamoto A (2009) Structural and functional basis of a role for CRKL in a fibroblast growth factor 8-induced feed-forward loop. *Mol Cell Biol* 29:3076–3087.
13. Guris DL, Fantes J, Tara D, Druker BJ, Imamoto A (2001) Mice lacking the homologue of the human 22q11.2 gene CRKL phenocopy neurocristopathies of DiGeorge syndrome. *Nat Genet* 27:293–298.
14. Tannour-Louet M, et al. (2010) Identification of de novo copy number variants associated with human disorders of sexual development. *PLoS One* 5:e15392.
15. San Agustin JT, et al. (2016) Genetic link between renal birth defects and congenital heart disease. *Nat Commun* 7:11103. Erratum in Nat Commun 7:11910.
16. Racedo SE, et al. (2015) Mouse and human CRKL is dosage sensitive for cardiac outflow tract formation. *Am J Hum Genet* 96:235–244.
17. George B, et al. (2014) Crk1/2 and CrkL form a hetero-oligomer and functionally complement each other during podocyte morphogenesis. *Kidney Int* 85:1382–1394.
18. Draaken M, et al. (2014) Classic bladder exstrophy: Frequent 22q11.21 duplications and definition of a 414 kb phenocritical region. *Birth Defects Res A Clin Mol Teratol* 100:512–517.
19. Tucker T, et al. (2013) Prevalence of selected genomic deletions and duplications in a French-Canadian population-based sample of newborns. *Mol Genet Genomic Med* 1:87–97.
20. Chen M, et al. (2006) Subtelomeric rearrangements and 22q11.2 deletion syndrome in anomalous growth-restricted fetuses with normal or balanced G-banded karyotype. *Ultrasound Obstet Gynecol* 28:939–943.
21. Boualia SK, et al. (2011) Vesicoureteral reflux and other urinary tract malformations in mice compound heterozygous for Pax2 and Emx2. *PLoS One* 6:e21529.
22. Hains DS, et al. (2010) High incidence of vesicoureteral reflux in mice with Fgfr2 deletion in kidney mesenchyma. *J Urol* 183:2077–2084.
23. Yu OH, Murawski IJ, Myburgh DB, Gupta IR (2004) Overexpression of RET leads to vesicoureteric reflux in mice. *Am J Physiol Renal Physiol* 287:F1123–F1130.
24. Bowen SE, Watt CL, Murawski IJ, Gupta IR, Abraham SN (2013) Interplay between vesicoureteric reflux and kidney infection in the development of reflux nephropathy in mice. *Dis Model Mech* 6:934–941.
25. Paredes J, et al. (2011) Assessing vesicoureteral reflux in live inbred mice via ultrasound with a microbubble contrast agent. *Am J Physiol Renal Physiol* 300: F1262–F1265.
26. Mechlin CW, Kogan BA (2014) What lessons can be learned from testicular histology in undescended testes? *Transl Androl Urol* 3:365–369.
27. Dutta S, Joshi KR, Sengupta P, Bhattacharya K (2013) Unilateral and bilateral cryptorchidism and its effect on the testicular morphology, histology, accessory sex organs, and sperm count in laboratory mice. *J Hum Reprod Sci* 6:106–110.
28. Fetting JL, et al. (2014) FOXD1 promotes nephron progenitor differentiation by repressing decorin in the embryonic kidney. *Development* 141:17–27.
29. Balikova I, Devriendt K, Fryns JP, Vermeesch JR (2010) FOXD1 duplication causes branchial defects and interacts with the TFAP2A gene implicated in the branchio-oculo-facial syndrome in causing eye effects in zebrafish. *Mol Syndromol* 1:255–261.
30. Scambler PJ (2000) The 22q11 deletion syndromes. *Hum Mol Genet* 9:2421–2426.
31. Edelhoff S, Villacres EC, Storm DR, Disteche CM (1995) Mapping of adenylyl cyclase genes type I, II, III, IV, V, and VI in mouse. *Mamm Genome* 6:111–113.
32. Lopez-Rivera E, et al. (2017) Genetic drivers of kidney defects in the DiGeorge syndrome. *N Engl J Med* 376:742–754.
33. Abler LL, et al. (2011) A high throughput in situ hybridization method to characterize mRNA expression patterns in the fetal mouse lower urogenital tract. *J Vis Exp* 54: e2912.
34. Lan ZJ, Xu X, Cooney AJ (2004) Differential oocyte-specific expression of Cre recombinase activity in GDF-9-iCre, Zp3cre, and Msx2Cre transgenic mice. *Biol Reprod* 71:1469–1474.
35. Dobin A, et al. (2013) STAR: Ultrafast universal RNA-seq aligner. *Bioinformatics* 29: 15–21.
36. Love MI, Huber W, Anders S (2014) Moderated estimation of fold change and dispersion for RNA-seq data with DESeq2. *Genome Biol* 15:550.